Theor Chem Account (2008) 119:19–28
DOI 10.1007/s00214-006-0245-7

REGULAR ARTICLE

Determination of the absolute configuration of chiral molecules via density functional theory calculations of vibrational circular dichroism and optical rotation: The chiral alkane D_3-anti-trans-anti-trans-anti-trans-perhydrotriphenylene

P. J. Stephens · F. J. Devlin · S. Schürch · J. Hulliger

Received: 6 December 2006 / Accepted: 15 December 2006 / Published online: 3 February 2007

Abstract The Absolute configuration (AC) of the chiral alkane D_3-anti-trans-anti-trans-anti-trans-perhydrotriphenylene (PHTP), **1**, is determined by comparison of density functional theory (DFT) calculations of its vibrational circular dichroism (VCD) and optical rotation (OR) to the experimental VCD and OR of (+)−**1**, obtained in high enantiomeric excess using chiral gas chromatography. Conformational analysis of **1** demonstrates that the all-chair (CCCC) conformation is the lowest in energy and that other conformations are too high in energy to be significantly populated at room temperature. The B3PW91/TZ2P calculated IR spectrum of the CCCC conformation of **1** is in excellent agreement with the experimental IR spectrum, confirming the conformational analysis and demonstrating the excellent accuracy of the B3PW91 functional and the TZ2P basis set. The B3PW91/TZ2P calculated VCD spectrum of the CCCC conformation of S-**1** is in excellent agreement with the experimental VCD spectrum of (+)−**1**, unambiguously defining the AC of **1** to be S(+)/R(−). The B3LYP/aug-cc-pVDZ calculated OR of S-**1** over the range 589–365 nm has the same sign and dispersion as the experimental OR of (+)−**1**, further supporting the AC S(+)/R(−). Our results confirm the AC proposed earlier by Farina and Audisio. This study provides a further demonstration of the excellent accuracy of VCD spectra predicted using Stephens' equation for vibrational rotational strengths together with the ab initio DFT methodology, and further documents the utility of VCD spectroscopy in determining the ACs of chiral molecules.

Keywords Absolute configuration · Vibrational circular dichroism · Optical rotation · Perhydrotriphenylene

P. J. Stephens (✉) · F. J. Devlin
Department of Chemistry, University of Southern California, Los Angeles, CA 90089-0482, USA
e-mail: pstephen@usc.edu

S. Schürch · J. Hulliger
Department of Chemistry and Biochemistry, University of Bern, 3012 Bern, Switzerland

1 Introduction

D_3-anti-trans-anti-trans-anti-trans-perhydrotriphenylene, PHTP **1**, is a chiral molecule.

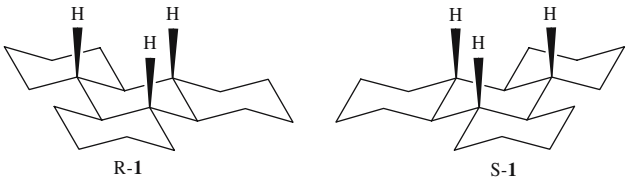

It was first synthesized in optically active form in 1967 by Farina and Audisio [1]. Racemic PHTP was converted to PHTP-carboxylic acid **2**, which was in turn resolved via its dehydro-abietylamine salt. Decarboxylation of (−)−**2** then led to (−)−**1**. The absolute configuration (AC) of (−)−**1** was assigned via calculation of its optical rotation using a Brewster method [2], leading to the AC R−(−). Subsequently, in 1970 [3], Farina and Audisio converted the carboxylic acid, **2**, to two bromo derivatives of **1** which were identified by NMR as the two epimers of 2-Br-PHTP, leading to the identification of **2** as 2-COOH-PHTP. (+)-**2** was converted to the 2-keto derivative of PHTP, (+)-**3**, whose optical

rotatory dispersion (ORD) and circular dichroism (CD) at ~290 nm exhibited a positive Cotton effect. Application of the Octant Rule [4] led to the assignment of the S AC to (+)−**3**. Since (−)-**2** yields (−)-**1** and (+)-**2** yields S-(+)-**3**, it follows that the AC of (-)−**1** is R, in agreement with the earlier assignment from the optical rotation. (−)-**1** of higher purity was also obtained with $[\alpha]_D = -93$ (methyl ethyl ketone), which was shown to be optically pure via isotopic dilution.

Racemic PHTP forms a rich variety of crystalline inclusion complexes [5,6] and the enantiomeric forms of PHTP can be expected to do likewise. In order to explore their inclusion complexes, a chromatographic method for the separation of the enantiomers of PHTP has recently been developed, giving optical purities of >99% in a single step [7]. Here, we take advantage of this development to re-investigate the AC of PHTP. The AC arrived at by Farina and Audisio is questionable for several reasons. First, the Brewster method for predicting optical rotations is empirical and has not proven to be of general reliability [8]. Thus, its use to assign the AC of PHTP is subject to considerable uncertainty. Second, the Octant Rule, used to analyze the ORD/CD of **3** is not 100% reliable. The incorrect assignment of the AC of the gyrochiral alkane, twistane, as a result of the application of the Octant Rule to precursor ketones provides a specific example of an erroneous outcome [9]. Thirdly, the identification of **3** as the 2-keto derivative of PHTP rests on the analysis of the NMR of the bromo derivatives obtained from **2**. Some possibility exists that substitution occurred at a different position on PHTP and that **3** is not the 2-keto derivative. Here, we re-investigate the AC of PHTP by comparing density functional theory (DFT) calculations of its vibrational circular dichroism (VCD) and optical rotation (OR) to experimental VCD and OR data. The application of DFT to the prediction of VCD spectra began in the early 1990s [10–15] and culminated in 1996 in the full-DFT implementation of Stephens' equation for vibrational rotational strengths [16] by Cheeseman et al. [15] Since 1998 this latter methodology has been commercially available via the GAUSSIAN program [17], leading to extensive usage of VCD spectroscopy in determining ACs [18–33]. The prediction of transparent spectral region OR and electronic circular dichroism (ECD) spectra using the time-dependent DFT (TDDFT) methodology was subsequently implemented within GAUSSIAN, making the use of OR and ECD for determining ACs more reliable than heretofore [34–42]. In this paper, we make use of the VCD and OR phenomena, together with DFT calculations, to definitively assign the AC of PHTP. ECD is not employed since the ECD of alkanes lies beyond the range of commercial ECD instruments.

2 Methods

(+)−**1** was obtained using gas chromatography, as described previously [7]. The enantiomeric excess (ee) was 93.5%.

IR and VCD spectra of a 0.0765 M CCl_4 solution of (+)−**1** were obtained using Nicolet MX-1 and Bomem/BioTools ChiralIR spectrometers, respectively. The latter instrument is equipped with a Dual Photo-Elastic Modulator accessory in order to reduce VCD artifacts, a methodology invented and implemented by Dr. J. C. Cheng at USC in 1975 [43]. Resolutions were 1 cm^{-1} (IR) and 4 cm^{-1} (VCD). VCD scan times were 1 h. IR and VCD spectra of CCl_4 provided baselines. A 597 μ pathlength KBr cell was used.

Experimental frequencies, dipole strengths and rotational strengths were obtained from the IR and VCD spectra via Lorentzian fitting [44–46] using the PeakFit software [47].

Conformational analysis (CA) of **1** was carried out as follows. The conformations of **1** were initially defined using Monte–Carlo searching, together with the MMFF94 force field, via the SPARTAN 02 program [48]. Geometry optimization of these conformations was then carried out using DFT via the GAUSSIAN 03 program [17].

Harmonic vibrational frequencies, dipole strengths and rotational strengths were calculated for the conformations predicted to be significantly populated at room-temperature using DFT via GAUSSIAN 03 [17]. Atomic Axial Tensors (AATs) are calculated using Gauge-Invariant (Including) Atomic Orbitals (GIAOs), guaranteeing origin-independent rotational strengths [15]. IR and VCD spectra were obtained from calculated frequencies, dipole strengths and rotational strengths using Lorentzian band shapes [44–46].

Specific rotations were calculated using TDDFT, together with GIAOs, via GAUSSIAN 03 [17].

3 Results

3.1 Conformational analysis

Monte-Carlo searching using the MMFF94 molecular mechanics force field and a 30 kcal/mol window found four inequivalent conformations **a**–**d**, with the relative energies given in Table 1. As anticipated, the lowest energy conformation **a**, is the all-chair conformation (CCCC). The other three conformations **b**–**d**, have one, two and three of the peripheral rings in boat conformations, respectively; all are substantially higher in energy than **a**. Reoptimization of the conformations **a**–**d** using

Table 1 Relative energies of the conformations of **1**

Conformer	ΔE^a (MMFF94)	ΔE^a (B3LYP/6-31G*)
a	0.00	0.00
b	4.72	4.28
c	9.94	10.07
d	15.45	17.02

[a] ΔE in kcal/mol

DFT at the B3LYP/6-31G* level leads to the relative energies given in Table 1. For **1**, B3LYP/6-31G* and MMFF94 relative energies are very similar (note that this is not always the case). Since the second lowest energy conformation, **b**, is >4 kcal/mol higher in energy than conformation **a**, we can safely conclude that at room temperature only **a** is significantly populated; i.e. PHTP is effectively a conformationally rigid molecule.

3.2 IR and VCD spectra

The mid-IR IR and VCD spectra of a 0.0765 M solution of (+)−**1** in CCl_4 were measured, with the results shown in Fig. 1. The baselines for the IR and VCD spectra were the spectra of neat CCl_4, measured under the same conditions. The ee of the (+)-PHTP sample was 93.5%. The VCD spectrum in Fig. 1 is normalized to 100% ee.

The VCD spectrum of (+)-PHTP exhibits an excellent signal-to-noise ratio and is significantly more structured than is the IR spectrum. It is also noteworthy that a substantial number of bands exhibit anisotropy ratios ($g = \Delta\varepsilon/\varepsilon$) $> 1 \times 10^{-3}$ (see Table 2 for the anisotropy ratios of all bands in the IR and VCD spectra): the largest anisotropy ratio is exhibited by the band at ~1,260 cm^{-1}, for which $g = 3.5 \times 10^{-3}$, an unusually large g value.

The harmonic vibrational frequencies, dipole strengths and rotational strengths of the all-chair conformation of S-**1** have been calculated using DFT, at the B3LYP/TZ2P and B3PW91/TZ2P levels, after reoptimization of the equilibrium geometry, with the results given in Table 2. Due to the D_3 symmetry of the CCCC conformation of **1** its vibrational modes are a_1, a_2 or e in symmetry; a_1 modes are forbidden. The IR and VCD spectra of **1**, obtained from the calculated frequencies, dipole strengths and rotational strengths using Lorentzian bandshapes [44–46] (with $\gamma = 4.0\,cm^{-1}$) are shown in Figs. 2 and 3, together with the corresponding experimental spectra. The B3LYP/TZ2P and B3PW91/TZ2P IR spectra are very similar, overall, but are not identical. For example, B3PW91 predicts modes 66/67 and 68/69 to be strong and very weak, respectively, whereas B3LYP predicts modes 68/69 to be stronger than 66/67. Comparison of the calculated and experimental IR spectra leads to the conclusion that the B3PW91 spectrum is in better agreement with experiment than is the B3LYP spectrum. In particular, the experimental band at ~1,210 cm^{-1} is narrow in bandwidth and shows no sign of the presence of more than one transition, consistent with the B3PW91 spectrum and inconsistent with the B3LYP spectrum. Accordingly, we base the assignment of the experimental spectrum on the B3PW91/TZ2P spectrum, with the results detailed in Fig. 2.

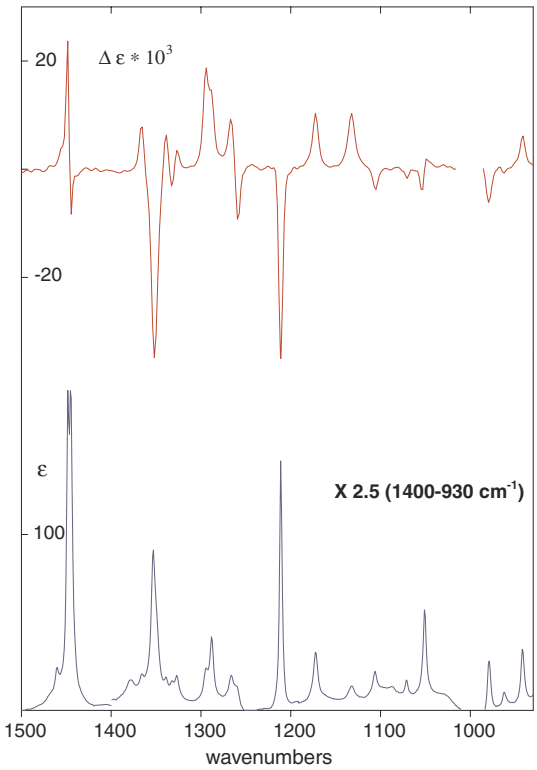

Fig. 1 The experimental IR and VCD spectra of (+)−**1** in CCl_4 solution (0.0765 M). The VCD spectrum is normalized to 100% ee

The B3LYP/TZ2P and B3PW91/TZ2P VCD spectra are also quite similar overall, but again they are not identical and the B3PW91 spectrum is in better agreement with experiment: see, for example, the tri-signate experimental bands at 1,320–1,340 cm^{-1}, which are excellently reproduced in the B3PW91 spectrum, but not in the B3LYP spectrum. The assignment of the experimental VCD spectrum based on the B3PW91/TZ2P spectrum is detailed in Fig. 3.

Having assigned the experimental IR and VCD spectra, we have then extracted the experimental frequencies, dipole strengths and rotational strengths via Lorentzian fitting, with the results given in Table 2. Examination of Table 2 shows that the assignments of the IR and VCD spectra are consistent: i.e. the IR

Table 2 Calculated and experimental frequencies, dipole strengths and rotational strengths of **1**

	Calculation						Experiment[a]						
	B3PW91/TZ2P			B3LYP/TZ2P			IR			VCD			
Mode	ν	*D*	*R*	ν	*D*	*R*	ν	*D*	γ	ν	*R*	γ	g[b]
108	1,501	4.0	0.2	1,511	3.0	–0.1							
							1,460	12.8	3.7				
107	1,501	4.0	0.2	1,511	3.0	–0.1							
106	1,500	0.0	0.0	1,510	0.0	0.0							
105	1,489	67.5	57.8	1,501	56.8	51.0	1,448	43.5	1.6	1,449	29.8	2.2	2.74
104	1,486	2.1	–12.8	1,498	2.7	–13.6							
103	1,486	2.1	–12.8	1,498	2.7	–13.6							
102	1,483	11.2	–24.9	1,494	11.2	–22.8	1,445	65.8	2.1	1,445	–17.2	2.2	–1.05
101	1,482	22.9	8.9	1,494	19.1	10.1							
100	1,482	22.9	8.9	1,494	19.2	10.1							
99	1,478	0.8	–1.9	1,490	0.6	–1.4							
										1,437	–1.3	2.3	
98	1,478	0.8	–1.9	1,490	0.6	–1.4							
97	1,476	0.0	0.0	1,489	0.0	0.0							
96	1,407	0.0	0.0	1,413	0.0	0.0							
95	1,399	0.3	4.4	1,405	0.1	2.4							
							1,366	4.0	4.6	1,366	19.3	3.4	19.30
94	1,399	0.3	4.4	1,405	0.1	2.4							
93	1,388	23.4	–57.7	1,392	23.1	–54.3							
92	1,383	0.0	3.5	1,387	0.9	6.5							
91	1,383	0.0	3.5	1,387	0.9	6.5	1,353	26.7	3.7	1,352	–78.3	4.0	–11.73
90	1,382	2.0	–19.5	1,385	1.0	–20.9							
89	1,382	2.0	–19.5	1,385	1.0	–20.9							
88	1,375	0.0	0.0	1,379	0.6	3.5							
87	1,371	0.0	1.2	1,378	0.0	1.5							
86	1,367	0.9	5.7	1,378	0.0	1.5				1,339	16.1	2.9	16.51
							1,340	3.9	6.3				
85	1,367	0.9	5.7	1,377	0.0	0.0							
84	1,363	1.1	–7.9	1,368	0.0	0.0							
							1,332	2.9	5.9	1,333	–6.4	2.6	–8.83
83	1,363	1.1	–7.9	1,368	1.3	3.8							
82	1,361	0.0	0.0	1,368	1.3	3.8							
81	1,357	1.6	6.2	1,366	0.3	–4.8							
							1,326	4.1	4.2	1,327	5.6	2.4	5.46
80	1,357	1.6	6.2	1,366	0.3	–4.8							
79	1,354	0.0	0.0	1,361	0.0	0.0							
78	1,321	0.5	–7.7	1,333	2.1	23.5							
77	1,321	0.5	–7.7	1,329	0.1	3.0	1,295	5.7	3.8	1,295	27.7	3.0	19.44
76	1,321	3.2	31.6	1,329	0.1	3.0							
75	1,315	5.7	17.4	1,325	5.4	9.0							
							1,288	8.5	2.6	1,289	19.7	3.0	9.27
74	1,315	5.7	17.4	1,325	5.4	9.1							
73	1,298	5.6	28.3	1,303	4.3	23.4	1,267	6.4	4.3	1,267	20.6	3.5	12.88
72	1,289	0.0	0.0	1,296	0.0	0.0							
71	1,287	0.1	–4.4	1,293	0.1	–4.3							
							1,261	1.9	2.5	1,259	–16.5	2.4	–34.74
70	1,287	0.1	–4.4	1,293	0.1	–4.3							
69	1,243	0.0	0.3	1,249	12.6	4.9							
68	1,243	0.0	0.2	1,249	12.6	4.8							
67	1,236	18.6	–32.3	1,240	8.8	–31.2							
							1,211	21.9	1.6	1,211	–50.0	2.2	–9.13
66	1,236	18.6	–32.2	1,240	8.8	–31.2							
65	1,220	0.0	0.0	1,222	0.0	0.0							
64	1,193	8.5	16.9	1,193	4.3	13.0	1,172	12.2	4.1	1,173	22.8	3.5	7.48
63	1,186	0.0	0.0	1,191	0.0	0.0							
62	1,177	0.1	0.5	1,189	2.7	8.6							
61	1,153	2.4	16.4	1,145	2.2	13.7							
							1,133	8.4	7.3	1,132	27.3	4.0	13.00
60	1,153	2.4	16.4	1,145	2.2	13.7							
59	1,124	2.5	–4.0	1,125	2.7	–4.4							
							1,106	9.6	5.4	1,106	–7.7	2.9	–3.21
58	1,124	2.5	–4.0	1,125	2.7	–4.4							

Table 2 continued

	Calculation						Experiment[a]						
	B3PW91/TZ2P			B3LYP/TZ2P			IR			VCD			
Mode	ν	*D*	*R*	ν	*D*	*R*	ν	*D*	γ	ν	*R*	γ	g[b]
57	1,117	0.0	0.0	1,103	0.0	0.0							
56	1,104	1.5	–0.5	1,093	1.0	–0.6							
							1,089	9.0	7.8	1,089	–0.2	2.2	–0.09
55	1,104	1.5	–0.5	1,093	1.0	–0.6							
54	1,089	0.9	–1.5	1,087	1.4	–1.9							
							1,071	5.9	4.8	1,070	–2.7	2.3	–1.83
53	1,089	0.9	–1.5	1,087	1.4	–1.9							
52	1,082	0.0	0.0	1,070	1.3	–12.0							
51	1,068	1.0	–12.1	1,069	8.2	7.9				1,054	–9.0	2.1	
50	1,066	10.0	4.9	1,069	8.2	7.9							
49	1,066	10.0	5.0	1,065	0.0	0.0							
							1,051	17.4	3.1	1,050	9.3	4.9	2.14
48	1,064	1.1	1.6	1,055	0.0	0.1							
47	1,064	1.1	1.6	1,055	0.0	0.1							
46	1,053	0.0	0.0	1,038	0.0	0.0							
45	992	12.4	–16.5	996	14.0	–17.5	979	5.5	1.6	979	–12.0	2.4	–8.73
44	979	3.1	–3.3	971	0.7	–0.3	962	2.0	2.1	962	–1.1	1.9	–2.20
43	957	5.0	6.8	947	5.7	6.4							
							942	7.2	1.8	942	16.6	3.5	9.22
42	957	5.0	6.8	947	5.7	6.4							

Frequencies ν in cm^{-1}; dipole strengths D in 10^{-40} esu^2 cm^2; rotational strengths R in 10^{-44} esu^2 cm^2; Lorentzian bandwidth parameters [44–46] γ in cm^{-1}. Experimental rotational strengths are for (+)−**1**; calculated rotational strengths are for (S)-**1**

[a] From Lorentzian fitting of the IR and the VCD spectra in Fig. 1

[b] Experimental anisotropy ratios $g = 4R/D$ in 10^{-4}

and VCD of all modes are at the same frequencies. The experimental frequencies, dipole strengths and rotational strengths are compared to the B3PW91/TZ2P calculated values in Figs. 4, 5, 6. The calculated frequencies are systematically higher than the corresponding experimental frequencies by 1–3%; as is well-known [49], these differences originate predominantly in the neglect of anharmonicity in the calculations of the frequencies. The calculated dipole and rotational strengths are in good agreement with the experimental parameters, strongly supporting the assignment of the IR and VCD spectra.

In comparing the calculated and experimental VCD spectra we have compared the calculated spectrum of S-**1** to the experimental spectrum of (+)−**1**. The excellent agreement of the calculated and experimental VCD spectra and rotational strengths demonstrates unambiguously that the absolute configuration (AC) of (+)−**1** is S. The VCD spectrum of R−**1** is the mirror-image of that of S-**1** and is completely inconsistent with the experimental spectrum of (+)−**1**. The AC of (+)−**1** cannot be R.

3.3 Optical rotation

The specific rotation [α] of (+)−**1** has been measured in CCl_4 solution at the sodium D line and at several mercury wavelengths, with the results, normalized to 100% ee, given in Table 3. With decreasing wavelength [α] increases monotonically.

The specific rotations of S-**1** at the wavelengths used experimentally have been calculated using TDDFT at the B3LYP/aug-cc-pVDZ//B3LYP/6-31G* level, with the results also given in Table 3. Calculated and experimental rotations are compared in Fig. 7. Qualitatively, calculated and experimental rotations are in agreement in sign and in dispersion, supporting the S-(+) AC of **1**. Quantitatively, calculated rotations are systematically greater than experimental rotations.

4 Discussion

The purpose of our study of PHTP is two-fold. The first objective is to definitively define its AC. The second is to further assess the quantitative reliability of Stephens' equation for vibrational rotational strengths [16], implemented using ab initio DFT.

Both goals are facilitated by the conformational rigidity of PHTP. As expected, both molecular mechanics and DFT calculations predict that the all-chair, CCCC, conformation is the lowest in energy. Conformations in which 1–3 rings are in boat conformations instead are substantially higher in energy, and therefore not significantly populated at room temperature. The prediction that only the CCCC conformation is populated is

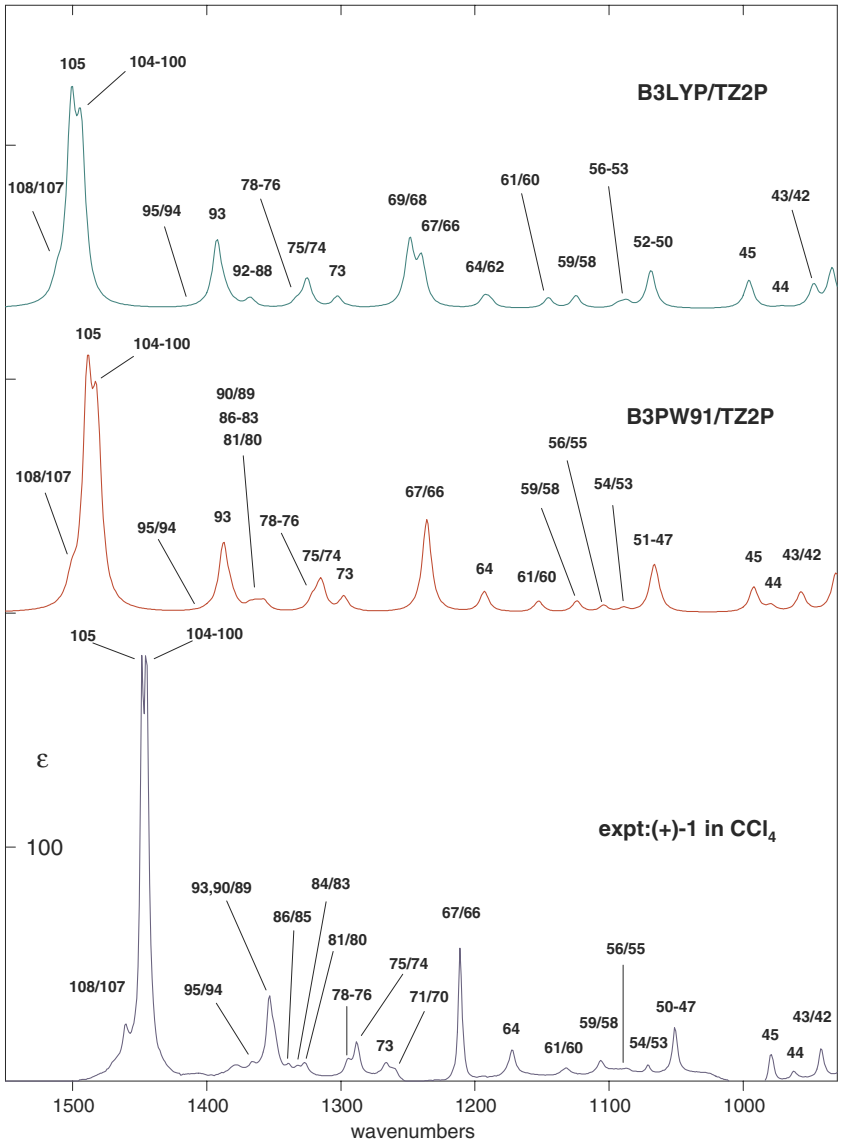

Fig. 2 Comparison of the B3LYP/TZ2P, B3PW91/TZ2P and experimental IR spectra of **1**. The bandshapes of the calculated spectra are Lorentzian ($\gamma = 4.0\,\mathrm{cm}^{-1}$). The numbers define the fundamental modes of **1** contributing to the spectral bands

strongly supported by the excellent agreement of the DFT-calculated IR and VCD spectra of this conformation with the experimental spectra. The IR and VCD spectra of PHTP have been calculated using the TZ2P basis set and the two hybrid density functionals B3LYP and B3PW91. The TZ2P basis set has been shown to be a good approximation to the complete basis set in predicting IR and VCD spectra [25]. B3LYP and B3PW91 are state-of-the-art hybrid functionals, the most accurate class of density functionals. We use two functionals in order to gauge the sensitivity of the calculated spectra to the choice of functional. In the case of PHTP, we have found B3LYP and B3PW91 to give similar, but not identical spectra, the B3PW91 spectra being in better agreement with experiment. Accordingly, our analyses of the IR and VCD spectra of PHTP are based on the B3PW91/TZ2P spectra.

The excellent agreement of the B3PW91/TZ2P IR and VCD spectra of PHTP with the experimental spectra leads to unambiguous assignment of the experimental spectra. In the case of the VCD spectra, agreement is obtained when the calculated spectrum of S-PHTP is compared with the experimental spectrum of (+)-PHTP, leading to the totally certain conclusion that the AC of PHTP is S-(+), the AC previously arrived at by Farina and Audisio [1,3].

To define the quantitative accuracy of the B3PW91/TZ2P IR and VCD spectra, we have compared the calculated frequencies, dipole strengths and rotational strengths of those transitions observed experimentally to the experimental values of these parameters. Fortunately, vibrational transitions of molecules in dilute solution in “innocuous” solvents (i.e. in which solute–solvent interactions are minimal) exhibit

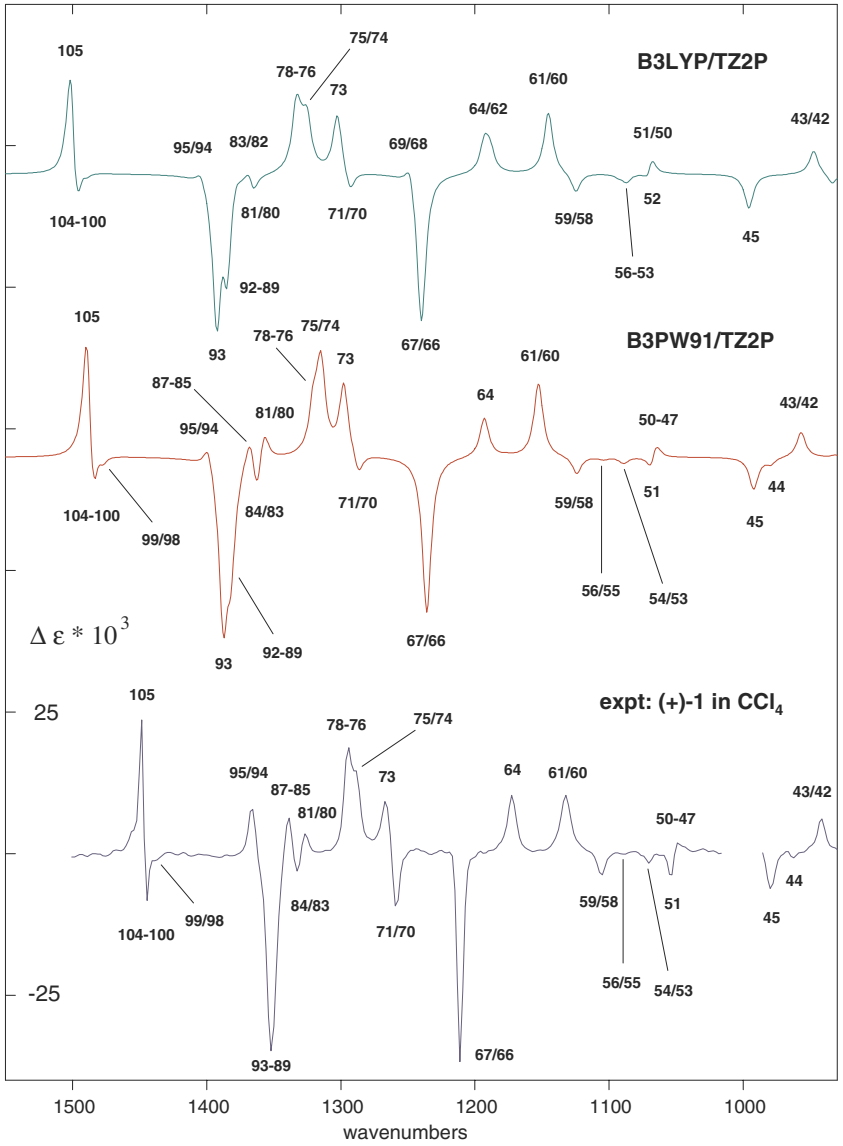

Fig. 3 Comparison of the B3LYP/TZ2P, B3PW91/TZ2P and experimental VCD spectra of **1**. The bandshapes of the calculated spectra are Lorentzian ($\gamma = 4.0\,\mathrm{cm}^{-1}$). The numbers define the fundamental modes of **1** contributing to the spectral bands

Lorentzian band shapes, and Lorentzian fitting provides accurate values of the experimental parameters. As shown in Figs. 4–6, the quantitative agreement of calculated and experimental frequencies, dipole strengths and rotational strengths is excellent. The differences can be attributed to : (1) the use of the harmonic approximation in the calculations, i.e. the neglect of anharmonicity; (2) the neglect of solvent effects; (3) the imperfection of the B3PW91 functional and the TZ2P basis set. The predominant contributor to the errors in the calculated frequencies is the neglect of anharmonicity [49]. Whether this is also the case for the calculated dipole and rotational strengths remains to be determined: this requires anharmonicity to be included in the DFT calculation of these parameters. Given the absence of specific solute–solvent interactions in CCl_4 solutions of PHTP, solvent effects are almost certainly very small. Lastly, given the difference in the IR and VCD spectra of PHTP calculated using the B3PW91 and B3LYP functional, it is likely that B3PW91 is not perfect, and that the future development of more accurate functionals will significantly reduce the differences between calculated and experimental spectra.

Critical to the accurate prediction of VCD spectra, using Stephens' equation, are the use of DFT, hybrid density functionals and a basis set which is a good approximation to the complete basis set. The only ab initio methodology available and practicable for the calculation of VCD in addition to DFT is the Hartree–Fock (HF) method. In Figs. 8 and 9 we compare rotational strengths calculated at the HF/TZ2P and B3PW91/6-31G* levels for S-**1** to the experimental rotational

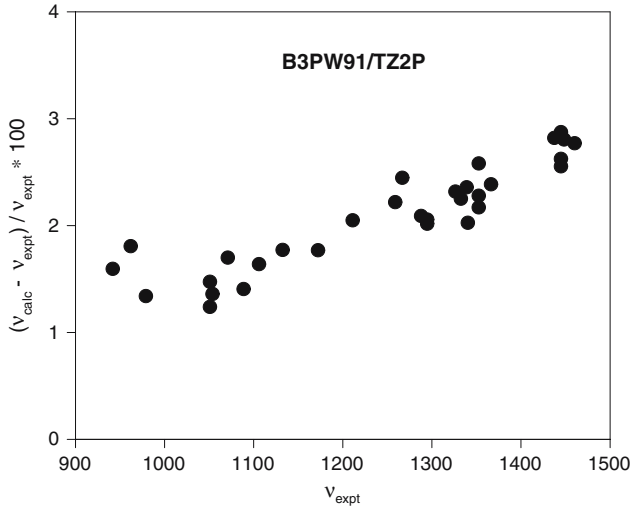

Fig. 4 Comparison of the B3PW91/TZ2P and experimental frequencies. For bands assigned to multiple vibrational modes, all calculated frequencies are compared to the corresponding experimental frequencies

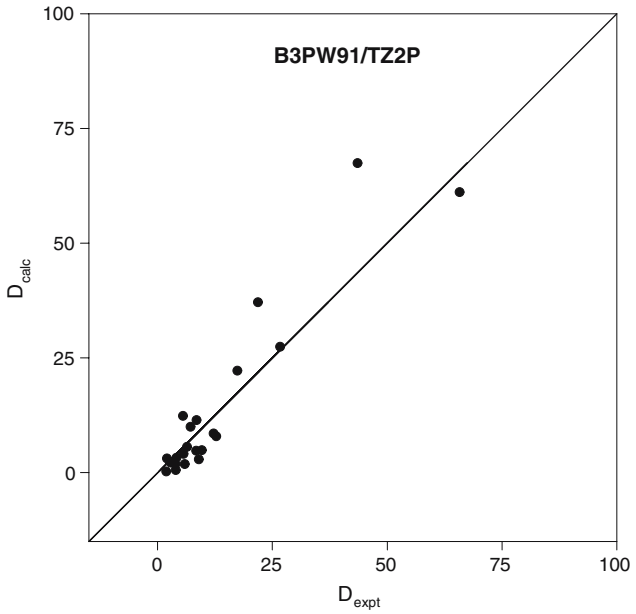

Fig. 5 Comparison of the B3PW91/TZ2P and experimental dipole strengths. For bands assigned to multiple vibrational modes, calculated dipole strengths are the sums of the dipole strengths of contributing modes. The *straight line*, of slope +1, is the "line of perfect agreement"

strengths for (+)−**1**. The scatter of the data in Figs. 8 and 9 from the "line of perfect agreement" is clearly greater than that in Fig. 6, unambiguously demonstrating the superiority of DFT with hybrid functionals over HF, and of the TZ2P basis set over 6-31G*. Quantitative comparison of the accuracies of the B3PW91/TZ2P, B3PW91/6-31G* and HF/TZ2P rotational strengths is

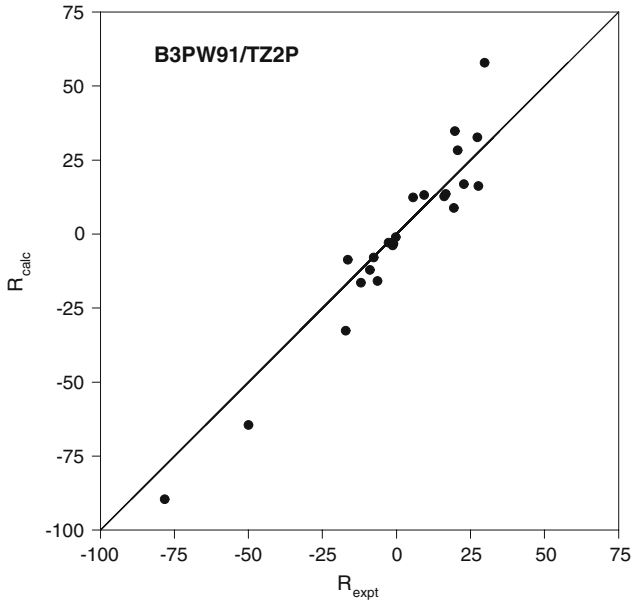

Fig. 6 Comparison of the B3PW91/TZ2P and experimental rotational strengths. For bands assigned to multiple vibrational modes, calculated rotational strengths are the sums of the rotational strengths of contributing modes. The *straight line*, of slope +1, is the "line of perfect agreement"

Table 3 Calculated and experimental specific rotations of **1**

λ (nm)	[α] (calc) [a]	[α] (expt)[b]
589	120.10	67.51
578	125.38	70.57
546	142.46	80.04
436	240.71	135.85
365	376.69	211.15

[a] [α] calculated for S-**1** at the B3LYP/6-31G* geometry using the aug-cc-pVDZ basis set and the B3LYP functional
[b] Normalized to 100% ee (c = 0.77, CCl_4)

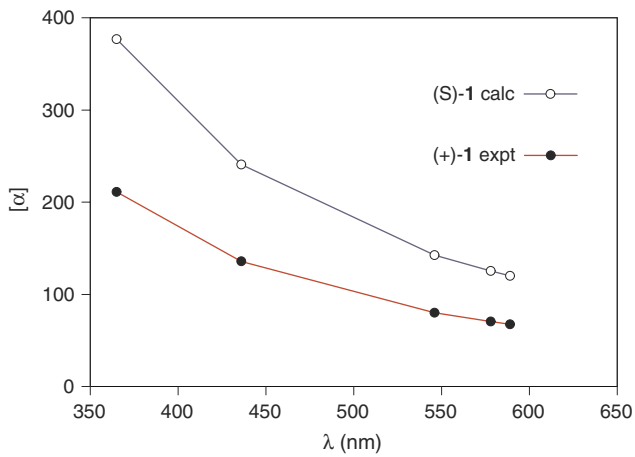

Fig. 7 B3LYP/aug-cc-pVDZ//B3LYP/6-31G* [α] values for S-**1** and experimental [α] values for (+)−**1**

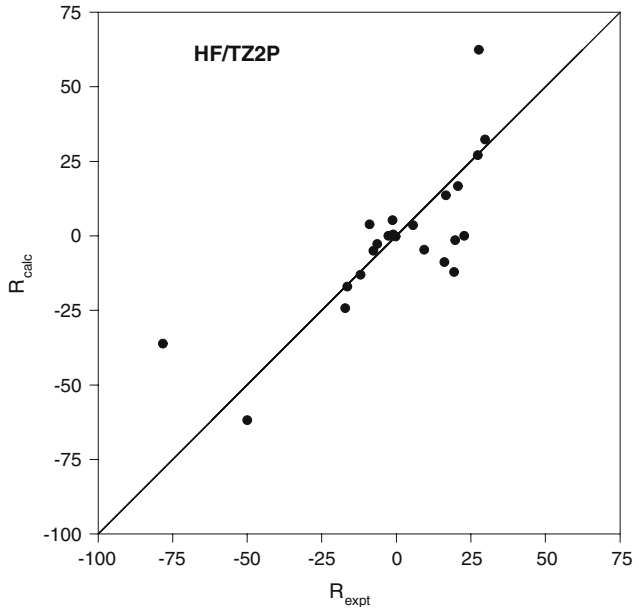

Fig. 8 Comparison of the HF/TZ2P and experimental rotational strengths. The *straight line*, of slope +1, is the "line of perfect agreement"

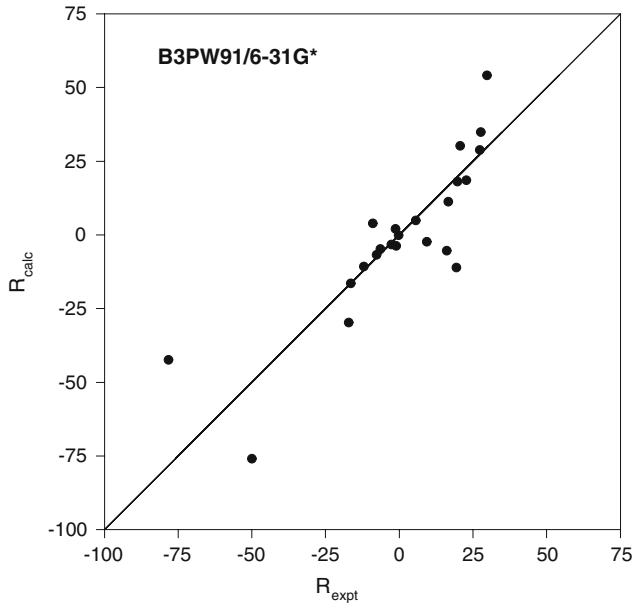

Fig. 9 Comparison of the B3PW91/6-31G* and experimental rotational strengths. The *straight line*, of slope +1, is the "line of perfect agreement"

detailed in Table 4. The mean absolute deviations, RMS deviations and "relative scatter ratios" all increase in the order B3PW91/TZ2P < B3PW91/6-31G* < HF/TZ2P, showing that, for **1**, the deterioration of the accuracy of the calculated rotational strengths is greater when DFT with the B3PW91 functional is replaced by the HF method than when the TZ2P basis set is replaced by 6-31G*.

Table 4 Comparison of VCD calculational methods

Method[a]	Mean absolute deviation[b]	RMS deviation[c]	Relative scatter ratio[d]
B3PW91/TZ2P	7.5405	9.8555	1.0000
B3PW91/6-31G*	9.3879	14.1712	1.6078
HF/TZ2P	11.0170	16.4465	2.5656

[a] Method used to calculate the rotational strengths
[b] Average of the absolute deviations of calculated rotational strengths from the experimental rotational strengths
[c] RMS deviation of calculated and experimental rotational strengths
[d] The average of the ratios of absolute deviations of calculated and experimental rotational strengths for the method used in the calculation to the absolute deviations for the B3PW91/TZ2P method. This parameter provides a quantitative measure of the increase in scatter from the "line of perfect agreement" of the data points in the plot of calculated versus experimental rotational strengths over the scatter of the B3PW91/TZ2P data

While the TDDFT specific rotations of **1** are in poorer quantitative agreement with experiment than are the DFT rotational strengths, the qualitative agreement of calculated and experimental rotations provides additional support for the AC derived from the VCD spectrum.

Acknowledgments We are grateful for financial support of this work from the National Science Foundation (Grants CHE-0209957 and CHE-0614577 to P.J.S.). We also thank the USC High Performance Computing and Communication (HPCC) facility for computer time and Dr. Jim Cheeseman of Gaussian Inc. for his continual assistance and advice.

References

1. Farina M, Audisio G (1967) Tetrahedron Lett 1285–1288
2. Brewster JH (1959) J Am Chem Soc 81:5475–5483
3. Farina M, Audisio G (1970) Tetrahedron 26:1827–1837 and 1839–1844
4. Lightner DA, Gurst JE Organic conformational analysis and stereochemistry from circular dichroism spectroscopy, Chap. 4, pp 63–94
5. Hoss R, König O, Kramer-Hoss V, Berger U, Rogin P, Hulliger J (1996) Angew Chem Int Ed Engl 35:1664–1666
6. König O, Bürgi HB, Armbruster T, Hulliger J, Weber T (1997) J Am Chem Soc 119:10632–10640
7. Schürch S, Saxer A, Claude S, Tabacchi R, Trusch B, Hulliger J (2001) J Chromatog A 905:175–182
8. Berson JA, Walia JS, Remanick A, Suzuki S, Reynolds-Warnhoff P, Willner D (1961) J Am Chem Soc 83:3986–3997
9. McCann DM, Stephens PJ, Cheeseman JR (2004) J Org Chem 69:8709–8717
10. Stephens PJ, Devlin FJ, Chabalowski CF, Frisch MJ (1994) J Phys Chem 98:11623–11627
11. Stephens PJ, Devlin FJ, Ashvar CS, Chabalowski CF, Frisch MJ (1994) Faraday Discuss 99:103–119

12. Bak KL, Devlin FJ, Ashvar CS, Taylor PR, Frisch MJ, Stephens PJ (1995) J Phys Chem 99:14918–14922
13. Devlin FJ, Finley JW, Stephens PJ, Frisch MJ (1995) J Phys Chem 99:16883–16902
14. Stephens PJ, Devlin FJ, Ashvar CS, Bak KL, Taylor PR, Frisch MJ (1996) In: Laird BB, Ross RB, Ziegler T (eds) Chemical applications of density-functional theory, ACS symposium series, vol 629, pp 105–113
15. Cheeseman JR, Frisch MJ, Devlin FJ, Stephens PJ (1996) Chem Phys Lett 252:211–220
16. Stephens PJ (1985) J Phys Chem 89:748–752
17. GAUSSIAN, Gaussian Inc., http://www.gaussian.com
18. Ashvar CS, Stephens PJ, Eggimann T, Wieser H (1998) Tetrahedron: Asymmetry 9:1107–1110
19. Aamouche A, Devlin FJ, Stephens PJ (1999) Chem Commun 361–362
20. Stephens PJ, Devlin FJ (2000) Chirality 12: 172–179
21. Aamouche A, Devlin FJ, Stephens PJ (2000) J Am Chem Soc 122:2346–2354
22. Aamouche A, Devlin FJ, Stephens PJ, Drabowicz J, Bujnicki B, Mikolajczyk M (2000) Chem Eur J 6:4479–4486
23. Stephens PJ, Aamouche A, Devlin FJ, Superchi S, Donnoli MI, Rosini C (2001) J Org Chem 66:3671–3677
24. Devlin FJ, Stephens PJ, Scafato P, Superchi S, Rosini C (2001) Tetrahedron: Asymmetry 12:1551–1558
25. Stephens PJ, Devlin FJ, Aamouche A (2002) In: Hicks JM (ed) Chirality: physical chemistry, ACS symposium series, vol 810, Chap. 2, pp 18–33
26. Devlin FJ, Stephens PJ, Scafato P, Superchi S, Rosini C (2002) Chirality 14:400–406
27. Devlin FJ, Stephens PJ, Oesterle C, Wiberg KB, Cheeseman JR, Frisch MJ (2002) J Org Chem 67:8090–8096
28. Stephens PJ (2003) In: Bultinck P, de Winter H, Langenaecker W, Tollenaere J (eds) Computational medicinal chemistry for drug discovery, Dekker, New York, Chap. 26, pp 699–725
29. Cere V, Peri F, Pollicino S, Ricci A, Devlin FJ, Stephens PJ, Gasparrini F, Rompietti R, Villani C (2005) J Org Chem 70:664–669
30. Stephens PJ, McCann DM, Devlin FJ, Flood TC, Butkus E, Stoncius S, Cheeseman JR (2005) J Org Chem 70:3903–3913
31. Devlin FJ, Stephens PJ, Besse P (2005) Tetrahedron: Asymmetry 16:1557–1566
32. Devlin FJ, Stephens PJ, Bortolini O (2005) Tetrahedron: Asymmetry 16:2653–2663
33. Carosati E, Cruciani G, Chiarini A, Budriesi R, Ioan P, Spisani R, Spinelli D, Cosimelli B, Fusi F, Frosini M, Matucci R, Gasparrini F, Ciogli A, Stephens PJ, Devlin FJ (2006) J Med Chem 49:5206–5216
34. Stephens PJ, Devlin FJ, Cheeseman JR, Frisch MJ, Mennucci B, Tomasi J (2000) Tetrahedron: Asymmetry 11:2443–2448
35. Stephens PJ, Devlin FJ, Cheeseman JR, Frisch MJ (2001) J Phys Chem A 105:5356–5371
36. Stephens PJ, Devlin FJ, Cheeseman JR, Frisch MJ (2002) Chirality 14:288–296
37. Stephens PJ, Devlin FJ, Cheeseman JR, Frisch MJ, Rosini C (2002) Org Lett 4:4595–4598
38. Stephens PJ, Devlin FJ, Cheeseman JR, Frisch MJ, Bortolini O, Besse P (2003) Chirality 15:S57-S64
39. McCann DM, Stephens PJ, Cheeseman JR (2004) J Org Chem 69:8709–8717
40. Stephens PJ, McCann DM, Butkus E, Stoncius S, Cheeseman JR, Frisch MJ (2004) J Org Chem 69:1948–1958
41. Stephens PJ, McCann DM, Devlin FJ, Cheeseman JR, Frisch MJ (2004) J Am Chem Soc 126:7514–7521
42. McCann DM, Stephens PJ (2006) J Org Chem 71:6074–6098
43. Cheng JC, Nafie LA, Stephens PJ (1975) J Opt Soc Am 65:1031–1035
44. Kawiecki RW, Devlin FJ, Stephens PJ, Amos RD, Handy NC (1988) Chem Phys Lett 145:411–417
45. Devlin FJ, Stephens PJ, Cheeseman JR, Frisch MJ (1997) J Phys Chem A 101:6322–6333
46. Devlin FJ, Stephens PJ, Cheeseman JR, Frisch MJ (1997) J Phys Chem A 101:9912–9924
47. PeakFit 4th ed.; Jandel Scientific Software: (1995)
48. Spartan 02; Wavefunction, Inc., http://www.wavefun.com
49. Finley JW, Stephens PJ (1995) J Mol Struct (Theochem), 357:225–235